CRAMÉR-RAO BOUNDS FOR RADAR ALTIMETER WAVEFORMS

Corinne Mailhes[(1)], *Jean-Yves Tourneret*[(1)], *Jérôme Severini*[(1)], *and Pierre Thibaut*[(2)]

[(1)] University of Toulouse, IRIT-ENSEEIHT-TéSA, Toulouse, France
[(2)] Collecte Localisation Satellite (CLS), Ramonville Saint-Agne, France
{jerome.severini,corinne.mailhes,jean-yves.tourneret}@enseeiht.fr, pierre.thibaut@cls.fr

ABSTRACT

The pseudo maximum likelihood estimator allows one to estimate the unknown parameters of Brown's model for altimeter waveforms. However, the optimality of this estimator, for instance in terms of minimizing the mean square errors of the unknown parameters is not guarantied. Thus it is not clear whether there is some space for developing new estimators for the unknown parameters of altimetric signals. This paper derives the Cramér-Rao lower bounds of the parameters associated to Brown's model. These bounds provide the minimum variances of any unbiased estimator of these parameters, i.e. a reference in terms of estimation error. A comparison between the mean square errors of the standard estimators and Cramér-Rao bounds allows one to evaluate the potential gain (in terms of estimation variance) that could be achieved with new estimation strategies.

1. PROBLEM STATEMENT AND DATA MODEL

Altimeters such as Poseidon-2 on Jason-1 and Poseidon-3 on Jason-2 provide useful information regarding the sea surface around the Earth. Altimeters send pulses which are frequency linear modulated and transmitted toward the ocean surface at a given pulse repetition frequency. After reflection on the sea surface, these pulses are backscattered and received by the altimeter. The formation of the resulting altimeter echoes (also called return powers) is illustrated in figure 1 extracted from [1]. Three distinct regions can be highlighted in the received altimeter signal: the first region ("thermal noise only" region) corresponds to the thermal noise generated by the altimeter before any return of the transmitted signal from the ocean surface (figure 1-a). The second part called the "leading edge" region contains all information about the ocean surface parameter and the altimeter height (figure 1-b and -c). Finally, the last part of the received signal referred to as a "trailing edge" region (figure 1-d) is due to return power from points outside the pulse-limited circle. Altimeter signals can be used to estimate many interesting ocean parameters, such as the significant wave height or the range, using a retracking algorithm [2]. This estimation assumes the received altimeter waveform can be modeled accurately by Brown's model [3], [4]. A simplified formulation of Brown's model assumes that the received altimeter waveform is parameterized by three parameters: the amplitude P_u, the epoch τ and the significant wave height H. The resulting altimeter waveform denoted as $x(t)$ can be written

$$x(t) = \frac{P_u}{2}\left[1+\text{erf}\left(\frac{t-\tau-\alpha\sigma_c^2}{\sqrt{2}\sigma_c}\right)\right] e^{-\alpha\left(t-\tau-\frac{\alpha\sigma_c^2}{2}\right)} + P_n \quad (1)$$

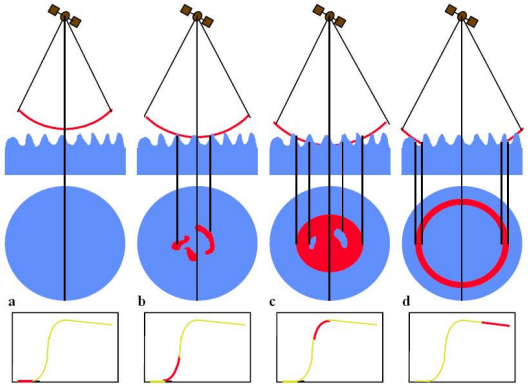

Fig. 1. Construction of a radar altimeter waveform.

where

$$\sigma_c^2 = \left(\frac{H}{2c}\right)^2 + \sigma_p^2,$$

$\text{erf}(t) = \frac{2}{\sqrt{\pi}}\int_0^t e^{-z^2}\,dz$ stands for the Gaussian error function, c denotes the light speed, α and σ_p^2 are two known parameters depending on the satellite and P_n is the instrument thermal noise. The retracking algorithm estimates the thermal noise from the first data samples and subtracts the estimate from (1). As a consequence, the additive noise P_n can be removed from the model (1) with very good approximation. The received signal $x(t)$ is sampled with the sampling period T_s, yielding

$$x_k = \frac{P_u}{2}\left[1+\text{erf}\left(\frac{u-\tau-\rho H^2}{\sqrt{2}\sqrt{\mu H^2+\sigma_p^2}}\right)\right] e^{v+\alpha\tau+\delta H^2}, \quad (2)$$

where $x_k = x(kT_s)$ and the following notations have been used

$$u = kT_s - \alpha\sigma_p^2, \quad v = -\alpha kT_s + \frac{\alpha^2\sigma_p^2}{2},$$
$$\rho = \frac{\alpha}{4c^2}, \quad \mu = \frac{1}{4c^2}, \quad \delta = \frac{\alpha^2}{8c^2}.$$

Figure 2 shows the waveform model and the influence of the three parameters P_u, τ and H. The epoch, τ corresponds to the central point of the "leading edge". The amplitude, P_u represents the amplitude of the waveform, while the significant wave height H is related to the slope of the "leading edge". Altimeter data are corrupted by multiplicative speckle noise. In order to reduce the influence of this noise affecting each individual echo, a sequence

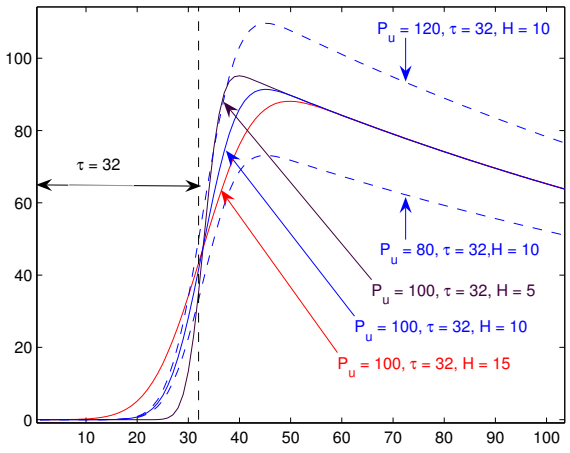

Fig. 2. Evolution of Brown's model as a function of the different parameters.

of L consecutive echoes are averaged on-board. Assuming pulse-to-pulse statistical independence [5], the resulting speckle noise denoted as n_k is distributed according to a gamma distribution whose shape and scale parameters equal the number of looks L (i.e. the number of incoherent summations of consecutive echoes). The observed waveforms can finally be written as

$$y_k = x_k n_k, \quad k = 0, ..., N-1. \tag{3}$$

Assuming independence between the observed altimeter samples, the joint distribution of $\mathbf{y} = (y_0, ..., y_{N-1})$ is

$$f(\mathbf{y}; \theta) = \frac{L^{NL}}{[\Gamma(L)]^N} \prod_{k=0}^{N-1} \frac{y_k^{L-1}}{x_k^L} \exp\left(-\sum_{k=0}^{N-1} \frac{L y_k}{x_k}\right), \tag{4}$$

where $\boldsymbol{\theta} = (P_u, \tau, H)$ is the parameter vector of interest. The maximum likelihood estimator (MLE) of $\boldsymbol{\theta}$ is classically obtained by differentiating the likelihood (4) with respect to the unknown parameters P_u, τ and H [6]. Due to the absence of closed-form expressions for the MLE of $\boldsymbol{\theta}$, pseudo-MLE solutions have been proposed in the literature [2]. The aim of this paper is to derive the Cramér-Rao bounds (CRB) of Brown's model parameters and to compare the mean square errors (MSEs) of the pseudo MLEs to these bounds. This comparison will help us to understand the potential gain in estimation performance we might obtain with other estimation algorithms than the classical pseudo-MLE. Indeed, when the MSE of an estimated parameter is close to its corresponding CRB, it is clearly not interesting to look for other estimation algorithms.

The paper is organized as follows: Section 2 details the main steps required to derive the CRBs of the three parameters defining Brown's model. Section 3 illustrates the behavior of these CRBs when key parameters are varying. A comparison between these bounds and the MSEs of the pseudo-MLEs is also presented. Section 4 generalizes the previous results to a more sophisticated model involving a fourth parameter referred to as off-nadir pointing angle. Conclusions are reported in Section 5.

2. CRAMÉR-RAO BOUNDS

The likelihood defined in (4) is denoted as f for brevity. The Fisher information matrix (FIM) for the unknown parameter vector $\boldsymbol{\theta}$ is given by

$$\boldsymbol{F} = -E\begin{bmatrix} \frac{\partial^2 \ln f}{\partial P_u^2} & \frac{\partial^2 \ln f}{\partial P_u \partial \tau} & \frac{\partial^2 \ln f}{\partial P_u \partial H} \\ \frac{\partial^2 \ln f}{\partial \tau \partial P_u} & \frac{\partial^2 \ln f}{\partial \tau^2} & \frac{\partial^2 \ln f}{\partial \tau \partial H} \\ \frac{\partial^2 \ln f}{\partial H \partial P_u} & \frac{\partial^2 \ln f}{\partial H \partial \tau} & \frac{\partial^2 \ln f}{\partial H^2} \end{bmatrix}, \tag{5}$$

where $E[.]$ stands for the mathematical expectation. The variance of any unbiased estimator of P_u, τ and H is bounded below by its corresponding Cramér-Rao bound (CRB) which is obtained by inverting the FIM (5). The unknown parameters P_u, τ, H are denoted by $\theta_1, \theta_2, \theta_3$. Any unbiased estimator of θ_1 denoted by $\widehat{\theta}_1$ satisfies the following inequality

$$\text{Var}\left(\widehat{\theta}_1\right) \geq \frac{-E\left(\frac{\partial^2 \ln f}{\partial \theta_2^2}\right) E\left(\frac{\partial^2 \ln f}{\partial \theta_3^2}\right) + \left[E\left(\frac{\partial^2 \ln f}{\partial \theta_2 \partial \theta_3}\right)\right]^2}{\det(\boldsymbol{F})}, \tag{6}$$

where $\det(\boldsymbol{F})$ is the determinant of $\boldsymbol{F}$. The right hand side of (6) is the CRB of θ_1. Of course, similar results are obtained for the other parameters θ_2 and θ_3 by exchanging indices. Determining the CRB of θ_1 requires to compute the expectations of the second order derivatives of f. It is straightforward to show that

$$E\left(\frac{\partial^2 \ln f}{\partial \theta_i \partial \theta_j}\right) = L \sum_{k=0}^{N-1} \frac{-1}{x_k^2} \frac{\partial x_k}{\partial \theta_i} \frac{\partial x_k}{\partial \theta_j}, \tag{7}$$

for $i, j = 1, 2, 3$, $(\theta_i, \theta_j) \in \{P_u, \tau, H\}^2$. The FIM elements of (5) can be computed using straightforward computations (details are available in the Appendix). As a result, the CRBs of the altimeter parameters P_u, τ and H can be expressed as

$$\begin{aligned} CRB(P_u) &= \frac{P_u^2}{L} \frac{\left(\sum G_k^2\right)\left(\sum M_k^2\right) - \left(\sum G_k M_k\right)^2}{\Delta} \\ CRB(\tau) &= \frac{1}{L} \frac{N\left(\sum M_k^2\right) - \left(\sum M_k\right)^2}{\Delta} \\ CRB(H) &= \frac{16c^4}{LH^2} \frac{N\left(\sum G_k^2\right) - \left(\sum G_k\right)^2}{\Delta} \end{aligned} \tag{8}$$

where G_k and M_k have been defined in the Appendix in (12), $\sum$ stands for $\sum_{k=0}^{N-1}$ and

$$\begin{aligned} \Delta = N\left(\Sigma G_k^2\right)\left(\Sigma M_k^2\right) + 2\left(\Sigma G_k\right)\left(\Sigma M_k\right)\left(\Sigma G_k M_k\right) \\ - \left(\Sigma G_k\right)^2\left(\Sigma M_k^2\right) - \left(\Sigma M_k\right)^2\left(\Sigma G_k^2\right) - N\left(\Sigma G_k M_k\right)^2. \end{aligned}$$

Two important observations can be made. First, the functions G_k and M_k defined in (12) do not depend on P_u (these terms only depend on the two other parameters τ and H). Therefore, the CRBs of τ and H are independent of the amplitude parameter P_u. This result can be explained by noting that the altimeter waveform x_k is corrupted by a multiplicative speckle noise.

A similar reasoning can be used to show that the CRB of P_u is a function of P_u^2. Second, all CRBs are inversely proportional to the number of looks L. The behavior of the three CRBs as a function of τ and H is not easy to analyze using (8) because G_k and M_k have too complex expressions (see (12)). This behavior will be illustrated in the next section.

3. NUMERICAL ILLUSTRATIONS

This section provides numerical results illustrating the CRB properties. Note that we do not study the influence of the number of samples N on these bounds since this parameter is fixed during the acquisition process. Figure 3 shows that the parameter CRBs are decreasing functions of the number of looks L. This result is not surprising since the number of looks is directly related to the noise level of the signal. Note that $L = 90$ in the Ku band for Poseidon-2 whereas $L = 15$ in the C band. This figure can also be used to derive the MSEs and the CRBs of the epoch in meters: in this case, the epoch corresponds to the distance between the satellite and the sea surface and it is denoted as d. Indeed, the epoch in meters is related to the epoch in seconds according to $d = \tau c/2$, hence, $\text{MSE}\left(\widehat{d}\right) = \text{MSE}\left(\widehat{\tau}\right) c^2/4$ (where $\widehat{d}$ and $\widehat{\tau}$ denote estimates of d and τ). As an example, for $L = 90$, we have $\text{MSE}\left(\widehat{\tau}\right) \approx -184$dB yielding $\sqrt{\text{MSE}\left(\widehat{d}\right)} \approx 9.8$cm. A similar computation leads to $\sqrt{CRB\left(d\right)} \approx 1.9$cm. Thus, the standard deviation of an optimal distance estimator is five times less than that of the MLE (i.e. corresponding to a gain of 8cm). Figures 4, 5 and 6 display the CRBs of the three parameters versus the different parameters. As already stated, Fig. 4 confirms that the CRBs of τ and H do not depend on amplitude values although the CRB of P_u is a quadratic function of this parameter. Figure 5 illustrates the slight influence of the epoch value on all CRBs. It can also be seen on figure 6 that the CRB for the estimation of the significant wave height, H, increases when H increases. These figures also compare the performance of the pseudo-MLE derived in [2] with the optimal MSEs provided by the CRBs. Note that the MSEs have been computed with 1000 Monte Carlo runs for synthetic signals defined by (3). It can be seen that the pseudo-MLE of the amplitude P_u is close to be optimal since its MSE is very close to the corresponding CRB. However, there is clearly some space for improving the estimation of the two other parameters τ and H.

4. BROWN'S MODEL WITH FOUR PARAMETERS

A more sophisticated and accurate model of the altimeter waveforms was proposed in [4] by introducing a fourth parameter in (2). The new parameter is the off-nadir pointing angle (denoted by ξ) which is mainly responsible for a slope change in the "trailing edge", corresponding to samples greater than 50 or 60 in Fig. 2. Several studies have shown that estimating this parameter is useful for the retracking algorithm [7], particularly in presence of blooms or rain cells. Of course, this fourth parameter induces some changes in Brown's model defined in (2). More precisely, P_u and α have to be modified as follows:

$$P_u \rightarrow P_u \exp\left(-\frac{4}{\gamma}\sin^2\xi\right),$$
$$\alpha \rightarrow \alpha\left[\cos\left(2\xi\right) - \frac{\sin^2\left(2\xi\right)}{\gamma}\right]. \quad (9)$$

The resulting CRBs of the four parameters can be derived, similarly to the case of three parameters. The FIM is now defined as a 4×4 matrix, whose elements are

$$F_{ij} = -E\left(\frac{\partial^2 \ln f}{\partial\theta_i \partial\theta_j}\right) \quad (10)$$

for $i, j = 1, ..., 4$ with $\theta_i \in \{P_u, \tau, H, \xi\}$. The analytical expressions of all FIM elements can be derived using (7). Note that the formulae given in the Appendix derived for three parameters can also be used for four parameters after replacing α in (12) and (13) by its new expression given in (9). Of course, this complicates significantly the CRB expressions which are not given in this paper for brevity (see [8] for details). However, the following comments are appropriate: 1) the CRBs in the case of four parameters are inversely proportional to the number of looks L (similarly to three parameters), as shown in Fig. 7, 2) the CRBs of τ, H and ξ are independent of P_u. The only bound which depends on P_u is the CRB of P_u itself that is still a quadratic function of P_u. Figure 7 also illustrates the loss of efficiency resulting from the estimation of four parameters instead of three. For example, for $L = 90$, we have $\sqrt{\text{MSE}\left(\widehat{d}\right)} \approx 21.2$cm and $\sqrt{CRB\left(d\right)} \approx 2.7$cm to be compared with the the results obtained before. The loss of estimation accuracy for parameter P_u, when moving from three parameters to four parameters, can be observed in Fig. 8. In particular, the pseudo-MLE of P_u is no-longer close to optimal when four parameters are used in Brown's model. Figures 9 and 10 display the CRBs for the four parameters as functions of the significant wave height and the off-nadir pointing angle. The MSEs of the pseudo-MLEs are also plotted in order to evaluate the estimation performance. It is interesting to note the behavior of the different CRBs are comparable to the three parameter case. However, the MLE of P_u seems to be less accurate for large values of H and/or ξ. This reinforces the idea that new estimators might be investigated even for the amplitude parameter. Moreover, if the estimation of ξ seems to be independent of H (see Fig. 9), the MLE does not behave quite well when ξ increases (see Fig. 10).

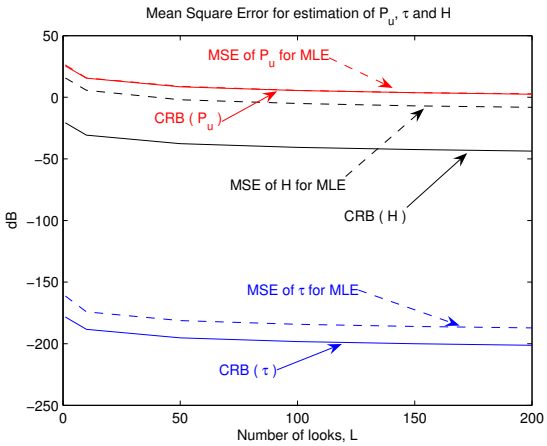

Fig. 3. CRBs and MSEs of the Pseudo-MLEs for the three parameters versus L ($P_u = 160, \tau = 32, H = 6$).

5. CONCLUSIONS

This paper derived Cramér-Rao lower bounds for the parameters of radar altimeter waveforms. These bounds have been obtained by assuming the altimetric signals satisfy Brown's model. A first study was conducted for the simplified model parameterized by the signal amplitude, the epoch and the significant wave height. A

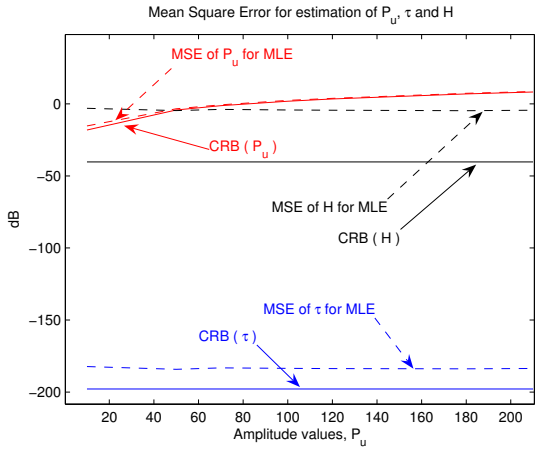

Fig. 4. CRBs and MSEs of the Pseudo-MLEs for the three parameters versus P_u ($L = 90, \tau = 32, H = 6$).

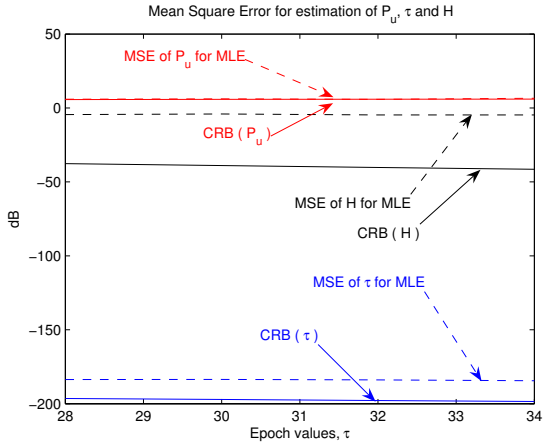

Fig. 5. CRBs and MSEs of the Pseudo-MLEs for the three parameters versus τ ($L = 90, H = 6, P_u = 160$).

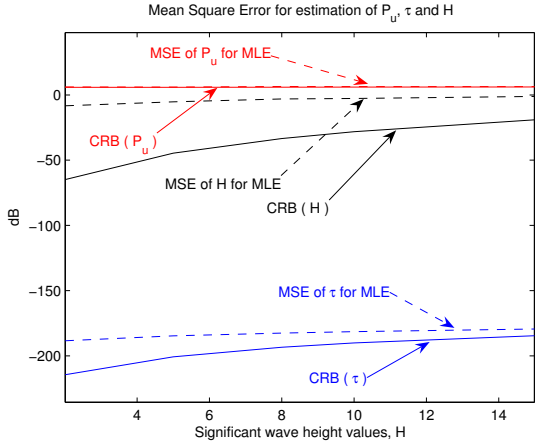

Fig. 6. CRBs and MSEs of the Pseudo-MLEs for the three parameters versus H ($L = 90, \tau = 32, P_u = 160$).

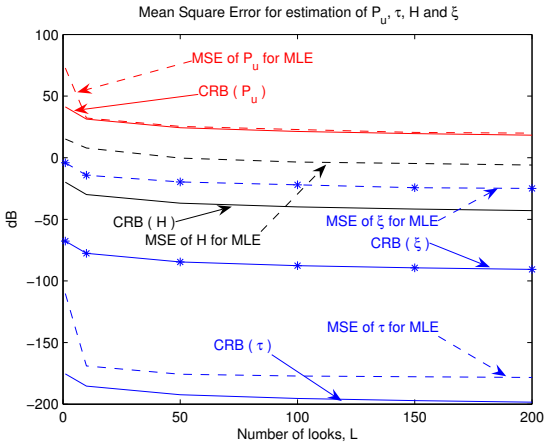

Fig. 7. CRBs and MSEs of the Pseudo-MLEs for the four parameters versus L ($H = 6, \tau = 32, P_u = 160, \xi = 0.1$).

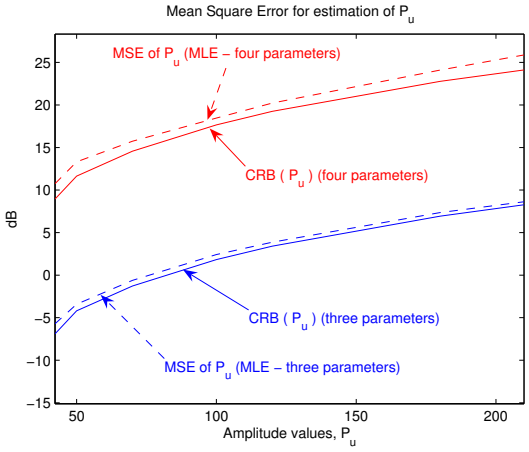

Fig. 8. Comparison between P_u estimates for three or four parameters in Brown's model ($L = 90, H = 6, \tau = 32, \xi = 0.1$).

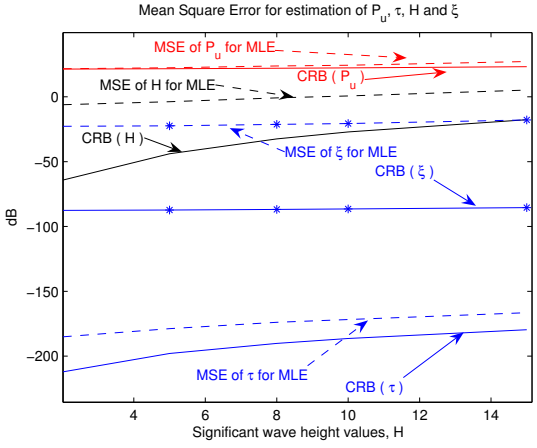

Fig. 9. CRBs and MSEs of the four parameter estimates versus H ($L = 90, \tau = 32, P_u = 160, \xi = 0.1$).

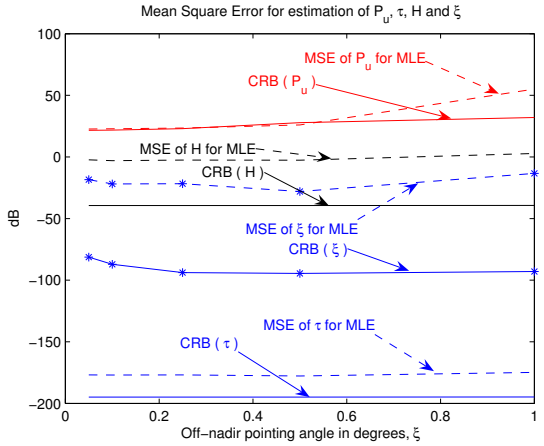

Fig. 10. CRBs and MSEs of the four parameter estimates versus ξ ($L = 90, \tau = 32, P_u = 160, H = 6$).

more accurate model including the off-nadir pointing angle as a fourth parameter was then considered. The obtained bounds were compared to the corresponding mean square errors of the pseudo maximum likelihood estimates. The main conclusion is that there is some space for improving the estimation of the epoch and the significant wave height. Conversely, the amplitude estimator is close to be optimal for the three parameter Brown's model. A significant loss of estimation performance was observed for the amplitude when the four parameter model is investigated.

Perspectives include the development of new estimation strategies for altimeter waveforms. The introduction of prior information regarding the different altimetric parameters through a Bayesian framework seems to be promising in this context [9]. Considering estimation strategies appropriate to waveforms which have been backscattered from non-oceanic surfaces (ices, deserts, ...) is also very challenging.

6. APPENDIX

Denote as F_{ij} the elements of the symmetric FIM. Equations (2) and (7) allow to compute the expectations of all second order derivatives:

$$\begin{aligned} F_{11} &= \tfrac{LN}{P_u^2} & F_{12} &= \tfrac{L}{P_u}\sum_{k=0}^{N-1} G_{k,\tau,H} \\ F_{22} &= L\sum_{k=0}^{N-1} G_{k,\tau,H}^2 & F_{13} &= \tfrac{L}{P_u}\tfrac{H}{4c^2}\sum_{k=0}^{N-1} M_{k,\tau,H} \\ F_{33} &= L\tfrac{H^2}{16c^4}\sum_{k=0}^{N-1} M_{k,\tau,H}^2 & F_{23} &= L\tfrac{H}{4c^2}\sum_{k=0}^{N-1} G_{k,\tau,H}M_{k,\tau,H} \end{aligned} \tag{11}$$

with

$$\begin{aligned} G_{k,\tau,H} &= \alpha - B_H\frac{\exp\left(-A_{k,\tau,H}^2\right)}{1+\operatorname{erf}\left(A_{k,\tau,H}\right)} \\ M_{k,\tau,H} &= \alpha^2 - D_{k,\tau,H}\frac{\exp\left(-A_{k,\tau,H}^2\right)}{1+\operatorname{erf}\left(A_{k,\tau,H}\right)} \end{aligned} \tag{12}$$

and

$$\begin{aligned} A_{k,\tau,H} &= \frac{kT_s - \tau - \frac{\alpha}{4c^2}H^2 - \alpha\sigma_p^2}{\sqrt{2}\sqrt{\frac{H^2}{4c^2}+\sigma_p^2}} \\ B_H &= \sqrt{\frac{2}{\pi\left(\frac{H^2}{4c^2}+\sigma_p^2\right)}} \\ D_{k,\tau,H} &= \sqrt{\frac{2}{\pi}}\frac{kT_s - \tau + \frac{\alpha}{4c^2}H^2 + \alpha\sigma_p^2}{\left(\frac{H^2}{4c^2}+\sigma_p^2\right)^{3/2}}. \end{aligned}$$

Note that the parameters $G_{k,\tau,H}$ and $M_{k,\tau,H}$ will be denoted as G_k and M_k for brevity.

In the case four parameters are considered, we use the following notations

$$V_{k,\tau,H,\xi} = I_{k,\tau,H,\xi} + B_H J_{H,\xi}\frac{\exp\left(-A_{k,\tau,H,\xi}^2\right)}{1+\operatorname{erf}\left(A_{k,\tau,H,\xi}\right)} \tag{13}$$

with

$$\begin{aligned} I_{k,\tau,H,\xi} = -2\sin(2\xi)\Bigg[\left(1+\frac{2}{\gamma}\cos(2\xi)\right)\Big(-\alpha k + \alpha\tau \\ + \left(\alpha^2\sigma_p^2 + 2\delta H^2\right)\left(\cos(2\xi) - \frac{\sin^2(2\xi)}{\gamma}\right)\Big) + \frac{2}{\gamma}\Bigg], \end{aligned}$$

and

$$J_{H,\xi} = 2\sin(2\xi)\left(1-\frac{2}{\gamma}\cos(2\xi)\right)\left(\alpha\sigma_p^2 + \rho H^2\right).$$

The FIM elements related to the ξ parameter can then be computed as follows

$$\begin{aligned} F_{14} &= \tfrac{L}{P_u}\sum_{k=0}^{N-1} V_{k,\tau,H,\xi} & F_{24} &= L\sum_{k=0}^{N-1} G_{k,\tau,H,\xi}V_{k,\tau,H,\xi} \\ F_{44} &= L\sum_{k=0}^{N-1} V_{k,\tau,H,\xi}^2 & F_{34} &= L\tfrac{H}{4c^2}\sum_{k=0}^{N-1} M_{k,\tau,H,\xi}V_{k,\tau,H,\xi}. \end{aligned} \tag{14}$$

The other FIM elements F_{ij}, $(i,j) \in \{1,2,3\}^2$ have the same expressions as in the three parameter case (11), except that α has to be modified as given by (9).

7. REFERENCES

[1] D. B. Chelton, J. C. Ries, B. J. Haines, L. L. Fu, and P. S. Callahan, *Satellite altimetry and Earth Sciences*. Academic Press, 2001.

[2] J.-P. Dumont, "Estimation optimale des paramètres altimétriques des signaux radar Poseidon," Ph.D. dissertation, Institut National Polytechnique de Toulouse, Toulouse, France, 1985.

[3] G. Brown, "Average impulse response of a rought surfaces and its applications," *IEEE Trans. Antennas and Propagation*, vol. 25, no. 1, pp. 67–74, Jan. 1977.

[4] G. Hayne, "Radar altimeter mean return waveforms from near-normal-incidence ocean surface scattering," *IEEE Trans. Antennas and Propagation*, vol. 28, no. 5, pp. 687–692, Sept. 1980.

[5] E. Walsh, "Pulse-to-pulse correlation in satellite radar altimeters," *Radio Science*, vol. 17, no. 4, pp. 786–800, Aug. 1982.

[6] S. Kay, *Fundamentals of statistical signal processing: estimation theory*. Englewood Cliffs, NJ: Prentice-Hall, 1993.

[7] L. Amarouche, P. Thibaut, O. Z. Zanife, J.-P. Dumont, P. Vincent, and N. Steunou, "Improving the Jason-1 ground retracking to better account for attitude effects," *Marine Geodesy*, vol. 27, pp. 171–197, 2004.

[8] J. Severini, "Cramér-Rao bounds for radar altimeter waveforms," Nov. 2007, University of Toulouse, internal report.

[9] J. Severini, C. Mailhes, P. Thibaut, and J.-Y. Tourneret, "Bayesian estimation of altimeter echo parameters," in *Proc. IEEE IGARSS*, Boston, MA, 2008, to appear.